The Abdus Salam
International Centre for Theoretical Physics

United Nations
Educational, Scientific and
Cultural Organization

IAEA
International Atomic Energy Agency

CEI
CENTRAL EUROPEAN INITIATIVE

2265-34

Advanced School on Understanding and Prediction of Earthquakes and other Extreme Events in Complex Systems

26 September - 8 October, 2011

Block structure modeling of the largest earthquakes at the SE Alps and Dinarides junction

I. Vorobieva
IIEP, Moscow
Russia

Block structure modeling of the largest earthquakes at the SE Alps and Dinarides junction

I. Vorobieva[1], A. Peresan[2], A. Soloviev[1], G.F. Panza[2,3]

[1]*International Institute of Earthquake Prediction Theory and Mathematical Geophysics. Russian Academy of Sciences. Profsoyuznaya 84/32, Moscow 117997, Russia.*

[2]*Department of Earth Sciences, University of Trieste, via E. Weiss 1, 34127 Trieste, Italy.*

[3]*The Abdus Salam International Centre for Theoretical Physics - SAND Group ICTP, 34100 Trieste, Miramare, Italy.*

Corresponding author:
I. Vorobieva

E-mail: vorobiev@mitp.ru

Tel: (7 495) 333 12 55

Fax: (7 495) 333 41 24

Abstract

The numerical model of block-structure dynamics is used to study the long-term characteristics of the strongest earthquakes at the SE Alps–Dinarides junction zone, consistently with historical observations. The fault-and-block geometry is outlined based on the morphostructural zoning and active faults map of the study area. The model reproduces the main features of the observed seismicity and kinematics in the region. In the synthetic earthquake catalog, which covers a time interval of 100,000 years, the average rate of the extreme events, with magnitude $M \geq 7$, is 1-2 per 1000 years, and the maximum magnitude is 7.4. Most of these events are located along the southern boundary of the Alps and a large group is located in Vinjdol-Rijeka zone. Several synthetic earthquakes with $M \geq 7$ are located along the Idrija line and at the eastern and western boundaries of northern Dinarides, which have experienced significant historical earthquakes with $M \geq 6$. The model delineates a number of possible locations for extreme events, where large earthquakes have not been observed in historical time; in particular at the western boundary of the Dinarides, nearby the city of Trieste. The results of modeling do not contradict the available historical observations and DISS3.1.1 data; hence they can be taken into account for a reliable and effective seismic hazard assessment of the study area.

Keywords: block structure model, strongest earthquakes, location, recurrence time, SE Alps - N Dinarides junction

1. Introduction

The estimation of seismic hazard and seismic risk assessment requires the identification of potentially hazardous zones, the estimation of recurrence period for destructive earthquakes and their maximum magnitude. The junction zone between SE Alps and N Dinarides is one of the most seismically active territories in Europe. A number of destructive events occurred here: the largest instrumentally recorded earthquake occurred in Friuli, 1976, and had magnitude 6.5. Such earthquakes expose to seismic hazard the north-eastern part of Italy (Friuli-Venezia-Giulia), Slovenia and Croatia, and specifically, the cities of Trieste, Udine and Ljubljana.

The region has a long history of seismicity monitoring and has been intensively studied in the last decade. Several catalogs of significant historical earthquakes that cover the zone of SE Alps-N Dinarides junction have been compiled: "Earthquake catalogue for Central and Southeastern Europe 342 BC - 1990 AD" (Shebalin et al., 1998), UCI (PERESAN AND PANZA, 2002), Catalogo Parametrico dei Terremoti Italiani (CPTI04) (GRUPPO DI LAVORO CPTI, 2004). A number of paleoseismicity studies have been carried out, as well. FITZKO et al. (2005) support the location of the epicenter of March 1511 earthquake reported by ŽIVČIČ et al. (2000) at the north of the Idrija line. A first order identification of the seismogenic nodes in Alps and Dinarides has been carried out by GORSHKOV et al. (2004), followed by a more detailed investigation where the geometry of each node in the Alps–Dinarides hinge zone is delineated and the recognition of seismogenic nodes is performed for earthquakes with $M \geq 6$ (GORSHKOV et al., 2009).

A significant progress in identification of seismically dangerous territories is reached by DISS working Group (data base 3.1.1 (2010)), (Basili et al, 2008, Caladini et al., 2005, Buratto et al., 2008, Vannoli et al., 2009, see diss.rm.ingv.it for more reference). A number of active faulting and modeling studies have been carried out; Bechtold et al. (2009) model active tectonics of the Friuli/NW Slovenia from CGPS measurement. Borghi et al., (2009) show through GPS monitoring an important amount of aseismic deformation related to the moderate-size earthquake Slovenian Krn Mountain earthquake. Slejko et al., (2011) demonstrate the contribution of "silent" faults to the seismic hazard of the northern Adriatic Sea.

In spite of these investigations, the reliable determination of the possible localization of the largest earthquakes, the estimation of their maximum magnitude and period of recurrence still remains an open problem. Available data cover more than one thousand years, nevertheless, the duration of instrumentally recorded catalogs spans several decades only. Historical catalogs based on the macroseismic observations and paleoseismic studies span a much longer time interval but they suffer from inhomogeneity and incompleteness. The accuracy of magnitudes is about ±0.6 for historical data (e.g. D'AMICO et al., 1998; SHEBALIN et al., 1998) and about ±0.3 for instrumental data, and epicenter determination may typically be not better than few tens of km (e.g. SUHADOLC et al., 1992; SHEBALIN et al., 1998). The progress in computer sciences and in the knowledge of earthquake physics permitted the development of a number of numerical models simulating seismicity that can be used to overcome, at least partially, the natural limits of observations.

In the present work we use the block structure model introduced by GABRIELOV et al. (1990) and described in detail by SOLOVIEV and ISMAIL-ZADEH (2003) to study strong seismicity in the zone of the Alps-Dinarides junction. In spite of the block structure model was developed in 90's, it still remains a powerful tool for different investigations (e.g. Peresan et al., 2007, Ismail-Zadeh et al., 2007,). The model is capable simulating both, geodynamics and seismicity. The main advantage of the model comparing with recently developed ones (e.g. Rundle, 2006) is its simplicity: basing on the hypothesis of the block structure of the Earth's lithosphere (Sadovskii, 1985) it is able to reproduce the integral features of regional seismicity and tectonic using relatively small number of input parameters. The previous studies demonstrate that block structure model can display correctly the possible location of strongest earthquakes, where they were not observed before: model of Sunda Arc (Soloviev and Ismail-Zadeh, 2003) generated

largest synthetic events in the zone of Sumatra, M=9.1, 2004, and model of Tibet-Himalaya (Ismail-Zadeh, et al. 2007) in the place where Sichuan, China M=7.9 earthquake occurred in 2008.
The present work deals with the study of the seismic regime at the SE Alps–Dinarides junction zone. The simultaneous analysis of the available observations and of the results of the numerical modeling allows us to get insights on the pattern of large earthquakes occurrence, i.e. the possible locations, maximum magnitude and recurrence period for future earthquakes.

2. Territory under study: instrumental and historical seismicity.

The study region includes Adria plate to the south, SE Alps to the north and N Dinarides to the east. The seismicity, from 1000 to 2011 with magnitude above 4.0 (PERESAN AND PANZA, 2002), the seismogenic sources (DISS3.1.1), the scheme of the morphostructural zoning (MSZ) (GORSHKOV et al., 2004), are shown in the Figure 1.

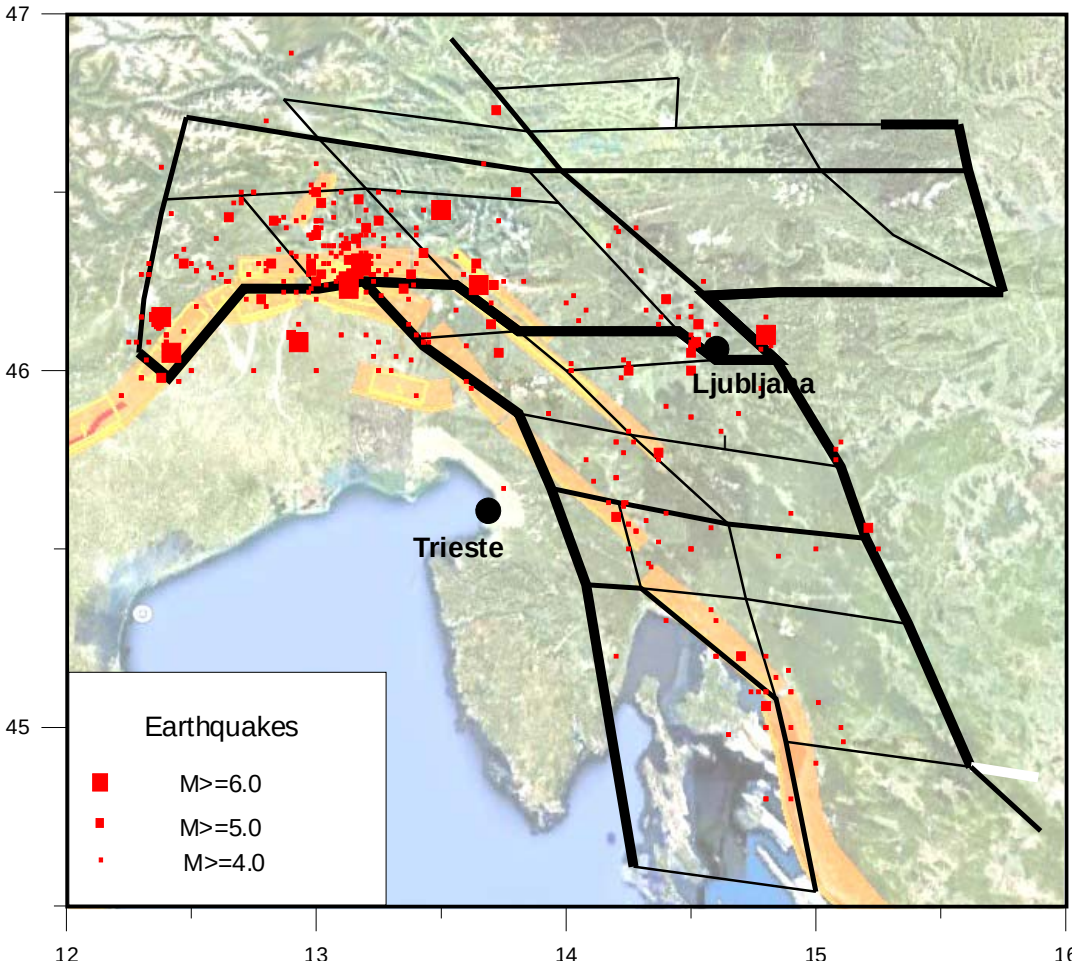

Fig. 1 Synoptic representation of the seismicity of the study region from 1000 to 2011 (PERESAN AND PANZA, 2002), the morphostructural zoning (GORSHKOV et al., 2004), and seismogenic sources (SS) (DISS3.1.1, 2010)): Orange bands are composite SS, yellow rectangles are individual SS. Black lines are morphostructural lineaments: Thick – I rank, medium – II rank, thin – III rank.

Several earthquake catalogs are available for the studied territory. As a main data set we use the catalog UCI (PERESAN AND PANZA, 2002) and its updates, referred in the following as UCI. It contains instrumentally recorded earthquakes as well as historical events, spanning a period of time from 1000 up to 2009, and covers completely the territory under study. The events with $M \geq 3.0$ are reported starting from 1870 for most of the territory, excluding its southern part, to the

south of latitude 45.5°, where earthquakes with magnitude in the range 3÷4.5 are systematically reported only after 1980. Before 1870 the catalog UCI contains historical data based essentially on macroseismic observations.

Besides the UCI catalog we analyze the historical large earthquakes reported in three other catalogs, namely: "Earthquake catalogue for Central and Southeastern Europe 342 BC - 1990 AD", (SHEBALIN et al., 1998) (ECCSE), "Catalogo Parametrico dei Terremoti Italiani (CPTI04)" (GRUPPO DI LAVORO CPTI, 2004) and the global NEIC catalog "Significant Earthquakes World Wide Data file". The ECCSE catalog does not cover a small portion of the studied territory to the west of longitude 13°E, while the other two catalogs cover completely the study region.

UCI, ECCSE, CPTI and NEIC catalogs report different sets of earthquakes with $M \geq 6.0$. All earthquakes with $M \geq 6.0$ at least in one of the four catalogs are listed in Table 1. The coordinates of epicenters and magnitudes given are those from the catalogs where the event is reported. In such a way a total of 21 large earthquakes are defined.

Table 1. Large earthquakes in the Alps-Dinarides junction region.

Date	*UCI*			*ECCSE*			*CPTI*			*NEIC*		
yyyy/mm/dd	*epicenter*		*M*	*epicenter*		*M*	*epicenter*		*M*	*epicenter*		*M*
567	-		-	45.60	15.30	**6.2**				45.6	15.3	-
792 2 1	-		-	46.00	14.50	**6.0**	-		-	-		-
1000 3 29	46.00	14.50	5.2	46.50	14.00	**6.9**	-		-	46.00	14.50	-
1097	-		-				45.60	15.30	**6.0**	-		-
1323	-		-	45.20	14.70	5.7	45.20	14.70	**6.0**	45.20	14.70	-
1348 1 25	46.33	13.43	5.7	46.50	13.60	**7.9**	46.25	12.88	**6.7**	46.40	13.50	-
1511 3 26	46.13	13.70	5.7	46.20	13.80	**7.4**	46.20	13.43	**6.5**	46.10	14.00	**6.9**
1511 8 8	46.05	13.73	5.7	46.10	13.40	**6.3**	-		-	46.10	13.40	-
1551 3 26	-		-	46.20	14.00	**6.3**	-		-	-		-
1690 12 4	46.73	13.72	5.2	46.50	13.90	**7.5**	46.63	13.87	**6.0**	46.60	13.80	-
1721 1 12	-		-	45.30	14.40	**6.1**	45.30	14.40	**6.0**	45.30	14.40	-
1870 3 1	-		-	45.50	14.50	**6.4**	45.40	14.40	5.6	-		-
1873 6 29	46.15	12.38	**6.3**	-		-	46.15	12.38	**6.3**	46.10	12.30	-
1895 4 14	46.13	14.53	5.6	46.05	14.50	**6.1**	46.13	14.53	**6.3**	46.10	14.50	**6.1**
1936 10 18	46.05	12.42	**6.2**	-		-	46.09	12.38	5.9	-		-
1963 5 19	46.10	14.80	**6.0**	46.04	14.84	4.8	46.10	14.80	5.2	46.00	14.60	**6.0**
1976 5 6	46.23	13.13	**6.5**	46.3	13.2	**6.5**	46.24	13.12	**6.4**	46.35	13.27	**6.5**
1976 6 17	46.08	12.93	**6.1**	-		-	-		-	46.16	12.86	**6.1**
1976 9 15	46.30	13.18	**6.0**	46.27	13.17	**6.0**	-		-	46.30	13.19	**6.3**
1976 9 15	46.25	13.13	**6.0**	46.28	3.14	5.9	46.25	13.12	5.9	46.30	13.10	**6.5**
1998 4 12	46.24	13.65	**6.0**	-		-	46.07	13.35	5.7	46.25	13.65	**6.0**

The MSZ scheme (GORSHKOV et al., 2004), and epicenter locations for the earthquakes listed in Table 1 are given in Figure 2A-D. All epicenters correlate well with the morphostructural lineaments that are traced independently from the existing information about seismicity (GORSHKOV et al., 2004 and 2009). The distribution of epicenters given by the different sources appears quite different, nevertheless it is possible to conclude the following: the most seismically active area in the region is the boundary SE Alps/N Dinarides and SE Alps/Friuli plain, especially the vicinity of triple junction of SE Alps, Dinarides and Adria. All the sources report several large events here: The instrumentally recorded large earthquakes Friuli, 1976, and Bovec, 1998 occurred here. The maximum level of recorded seismic activity is observed in this zone (see Figure 1) too. Another active zone is Vinjdol-Rijeka: three out of the four used sources report large earthquakes here; the level of instrumentally recorded seismicity is high as well. The information about large earthquakes at the Periadriatic line is less reliable: ECCSE gives magnitude M=7.5 and CPTI M=6.0 for the earthquake of 1690; some investigators (POSTPISCHL,

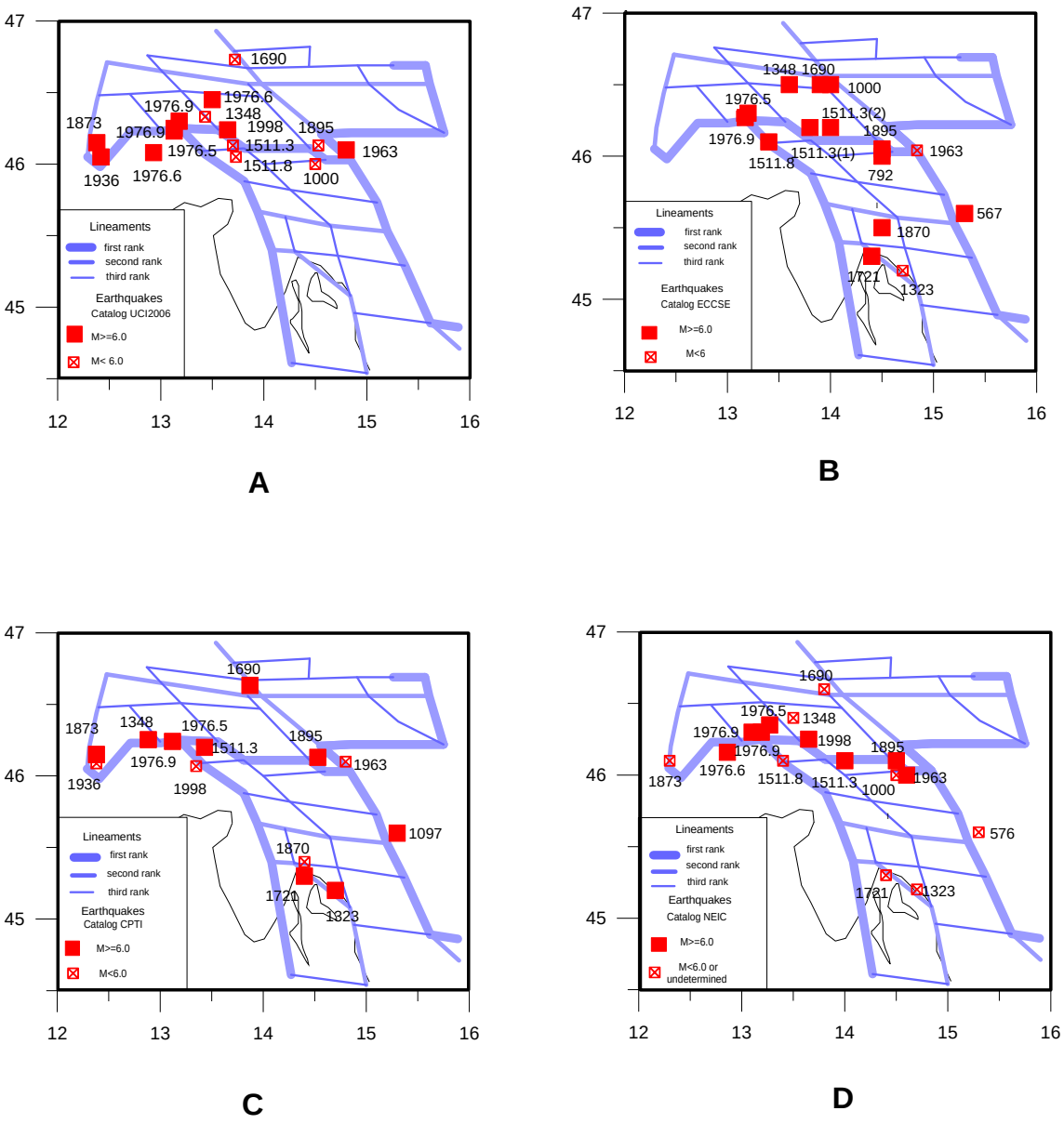

Fig. 2 Large earthquakes at the junction zone between Alps and Dinarides accordingly to the four sources of data available for this study: a - Catalog UCI, 1000 - 2011 (PERESAN AND PANZA, 2002); b - "Earthquake catalogue for Central and Southeastern Europe 342 BC - 1990 AD", (SHEBALIN et al., 1998); c - "Catalogo Parametrico dei Terremoti Italiani (CPTI04)", 1000 - 2004, (GRUPPO DI LAVORO CPTI, 2004); d - NEIC, Significant Earthquakes World Wide Data file, 500 – 2011

1985A, CAMASSI AND STUCCHI, 1996) place here the earthquake of 1348, but the uncertainty of its epicenter is very large (see table 1). The level of the instrumentally recorded seismicity is low.

The maximum instrumentally recorded magnitude is 6.5, Friuli 1976, and only one of the four considered sources, ECCSE, reports historical events with M>7 (Table 1). The maximum is M=7.9 (1348 event), but it seems overestimated, nevertheless, the equivalent magnitude of the instrumentally recorded Friuli series, 1976, calculated as

$$\log_{10}\left(\sum_{n} 10^{M_n}\right) = 7.04\,, \qquad (1)$$

where M_n is the magnitude of the n-th event as given in UCI turns out to be greater than 7. Therefore it is reasonable to conclude that the structure is able to generate earthquakes with magnitude 7 or greater.

3. Basic elements of the numerical block structure model

Formal description of the model. The realistic numerical modeling of block structure dynamics and seismicity was introduced by GABRIELOV et al. (1990) and described in details by SOLOVIEV AND ISMAIL-ZADEH (2003). The basic principles of the modeling are the follow. A block-structure is a limited and simply connected part of a layer, *d*, with thickness *H*, bounded by two horizontal planes. A region is formed by a system of rigid blocks that are separated by infinitely thin viscous-elastic fault planes. The boundaries of blocks can be as seismically active locked faults, as well "silent" slipping faults. Stresses and strain is concentrated at the fault planes and at the blocks bottoms.

The movement of the blocks is a consequence of the external motions that are prescribed at the segments of lateral confining boundaries, and at the bottom of the structure. The directions of these movements are assumed to be horizontal. The prescribed motions are assumed to be stationary and do not change during the modeling.

Elastic forces arise in the lower plane and in the fault planes as a result of the displacement of the blocks relative to the underlying medium, to the lateral boundary, and to the other blocks. The elastic stress at the point is proportional to the difference between the relative displacement and the slippage (the inelastic displacement) that is proportional to the elastic stress:

$$\mathbf{f} = K(\Delta\mathbf{r} - \delta\mathbf{r}), \quad \frac{d\delta\mathbf{r}}{dt} = W\mathbf{f}, \tag{2}$$

where **f** is the shear stress vector, $\Delta\mathbf{r}$ is the vector of relative displacement, and $\delta\mathbf{r}$ is the vector of slippage. Equations (2) correspond to visco-elastic (Maxwell) rheological law that describes the relation of stress **f** to the strain ζ

$$\left(\frac{d}{dt} + \frac{1}{\tau}\right)\mathbf{f} = \mu\frac{d\zeta}{dt} \tag{3}$$

here τ is the relaxation time ($\tau = \eta/\mu$), μ is the shear elastic modulus, and η is the viscosity. Coefficients in (2) and (3) are connected by formulas: $K = \mu/a$, $W = a/\eta$, where a is the actual width of the deforming zone, and $\tau = 1/(KW)$; μ, W, and τ are related to the one unit of the model time (ISMAIL-ZADEH et al., 2007), and the realistic estimation of the unit of time can be derived from the values of rheological parameters.

On the fault plane, the reaction force is normal to the fault plane and its size, per unit area, is:

$$|p_0| = |f_l \operatorname{tg} \alpha| \tag{4}$$

where f_l is the component of the elastic stress, **f**, normal to the fault on the upper plane, and α is the dip angle of the fault plane.

At each time moment the displacements of the blocks are found from the condition that the total force and the total moment of forces acting on each block are equal to zero. This is the condition of quasi-static equilibrium of the system and, at the same time, the condition of minimum energy.

The earthquakes are simulated in accordance with the dry friction model. When in a cell the ratio of shear to normal stress κ exceeds a prescribed value B (friction coefficient), an abrupt slippage occurs that drops κ to the given level H_f, ($H_f < B$). The new vector of the inelastic displacement $\delta\mathbf{r}^e$ is calculated:

$$\delta\mathbf{r}^e = \delta\mathbf{r} + \delta\mathbf{u}, \quad \delta\mathbf{u} = \gamma\mathbf{f} \tag{5}$$

where $\delta\mathbf{r}$ and **f** are just before the failure, and γ is determined from the condition that $\kappa = H_f$ after the failure, and new displacements of the blocks are determined to satisfy the condition of quasi-

static equilibrium. As a result κ can exceed critical level B in some other cells, this case the procedure is repeated till κ falls lower than B in the all cells. Each connected cluster of cells failured simultaneously forms as a single earthquake. Immediately after earthquake the rheological parameters change in the rapture cells; the rate of inelastic displacement increases considerably, and the parameter W_s ($W_s >> W$) is used instead of W in equation (2) as long as $\kappa > H_s$, ($H_s < H_f$); when κ decreases to H_s, the cell returns to the normal state.
The coordinates of the epicenter are determined as the geometrical center of mass of the raptured cells. The magnitude of the earthquake is calculated from Utsu and Seki, (1954):

$$Ms = 0.98 \log_{10} S + 3.93 \qquad (6)$$

where S is the total area of the cells forming the earthquake, measured in km^2 . Wells and Coppesmith (1994) give very similar relation Mw=0.98(±0.03) $\log_{10} S$ + 4.07(±0.06).
FPS of synthetic earthquake is determined as follows: strike and dip are prescribed by the block structure geometry, and rake is the direction of the slippage vector $\mathbf{\Delta U}$, as from (2) and (4) it follows that $\mathbf{\Delta U}$ lies in the fault plane where the earthquake occurs.

The input data for the modeling are: geometry of the block structure: fault network, dip angles of faults, and depth (thickness) of the structure; rates and directions of the tectonic motions at the lateral confining boundaries, and at the bottom of the structure; rheological parameters that describe the viscous-elastic features of the fault planes and block bottoms, and the conditions of earthquake occurrence.

The output of the modeling is the synthetic earthquake catalog (origin time, coordinates of epicenter, magnitude, and FPS), and the kinematics of the blocks: velocity field in the scale of the block size, and relative slip rate in the different fault zones.

Interpretation of the model assumptions. As any numerical modeling, the block structure model does not aim to reproduce the observations in all their details, since it assume a very simplified description of the study region**.**

1. *Rigid blocks*. This assumption means that we neglect the changes in the geometry of the block and fault's structure during the numerical simulation. It is justified by the fact that in the lithosphere the effective elastic moduli of the fault zones are significantly smaller than the ones within the blocks (e.g. Fialko, 2006, Barbot et al., 2009), and viscosity is 3-4 order smaller (e.g. Hacker et al,. 1992, McCafrey et al., 2000), i.e. ability of strain accumulation in the faults are zones is 3-4 order higher than within blocks, and fixed geometry is rather realistic for short (as compared with the geological history) periods of simulation: the rate of the tectonic motions is of the order of cm/yr or even mm/yr, and the linear size of the blocks is at least several tens of kilometers, thus the strain is small in the scale of the whole block structure.

As soon as we consider displacement in the scale of the fault's cells it turns out inhomogeneous along the fault plane, in spite of rigid blocks movement, as the inelastic displacement depends on the stress level and seismic history in the individual cell (Eq.(2)). This mechanism provides a stress transfer and its redistribution in the fault planes and block's bottoms, and can be interpreted as "stress shadows". It also explains why not only large earthquakes breaking the whole segment, but the small events as well have physical sense.

2. *Infinitely thin visco-elastic faults*. The fault zone (zone of strain accumulation) that in reality has width of several km, and a complex structure including many faults, is modeled as a single, infinitely thin plane; nevertheless, the difference in the fault zones features (e.g. width, viscosity, etc.) can be taken into account by proper choice of the rheological parameters.

3**.** *Horizontal motions***.** The tectonic motions prescribed at the lateral confining boundaries and at the bottom of the block structure are assumed to be horizontal, as well as the movements of blocks obtained as the result of the modeling. This assumption is supported by CUFFARO et al. (2006), who showed that the steady faster horizontal velocity of the lithosphere with respect to the upward or downward velocities at plate boundaries supports dominating tangential forces acting on plates. Nevertheless the model has three-dimensional features as any direction of

slippage is allowed in the fault planes with arbitrary dip angles, i.e. a relative displacement of blocks in a point of a fault plane can have a vertical component.

4. *Dimensionless time* is used while modeling. The relation between model and physical time is hidden in the in the rheological parameters and can be derived from (3). It depends on the viscosity and of the width of the fault zone. As the viscosity can't be measured directly, and estimation of its value can vary several orders, the interpretation of the unit of model time is a result of parametric tests. Nevertheless, it is possible to determine a set of rheological parameters that provide correspondence between tectonic velocities, earthquake productivity and realistic values of elastic shear modulus, viscosity, and the width of the fault zones. An example will be demonstrated in the present work below.

5. *Dip structure*. The model does not take into account the inhomogeneity that may be present at depths in the region, i.e. all the blocks have the same depth, and rheology of the fault zones does not chance with depth. The sort of average values is used for the entire fault segment in the model.

6. *Uncertainty of the input parameters*. Based on the available observations (structural and tectonic schemes of the region, GPS measurements, estimation of rheological features, etc…) the input parameters for the modeling can't be determined in a unique way, because the observations are incomplete, have limited accuracy, and are consistent with different interpretations. With alternating of the parameters the result of modeling can change. From the previous experience of the modeling we know that the model is sensitive to the prescribed motions and rheological parameters (Peresan et al., 2007, Soloviev et al, 1999), while the fragmentation of the fault network (scale of details) does not influence significantly the maximum magnitude and earthquake productivity (Keilis-Borok et al., 1997).

4. Block model of the Alps and Dinarides junction region

We determine the model parameters basing on the available knowledge about, tectonics, structure, fault's network, GPS observations in the studied area *No any information about observed seismicity is used for determination of parameters for modeling*.

Geometry. To outline the fault-and-block geometry we use the morphostructural zoning map of the Alps and Dinarides (GORSHKOV et al., 2004) it as, in the covered territory, it includes all active faults zones (Figure 1), as it provides blocks, and as the location of the known large earthquakes correlate petty well with the MSZ lineaments (Figure 2). The morphostructural zoning is based on the geological, morphological, and topographical analysis of the territory, and do not use any information about seismicity. For the details and evidences of MSZ in the studied region we address reader to original paper (GORSHKOV et al., 2004, and 2009). We also use the map active faults (DISS3.1.1), almost all seismogenic sources fit to MSZ scheme. We trace the faults of the block structure along all lineaments of the first and second rank, and also lineaments of the third rank those that are seismogenic sources in DISS3.1.1 (Idrija line), and to bound the block structure to the south. The block structure consists of six blocks that are outlined by sixteen faults (Figure 3). Two blocks in the north (B1, B2) represent the SE Alps. Four southern blocks (B3 - B6) represent the N Dinarides.

Two structural boundaries could be distinguished, at depth, in the study region (CHIMERA et al., 2003; PANZA AND RAYKOVA, 2008): the first one is the Moho discontinuity at a depth of about 40 km (e.g. CLOETINGH et al., 2006) and another structural boundary (Conrad discontinuity) is seen at a depth of about 20-25 km. Thus, the available information suggests fixing the thickness of the block structure either at 40 km or 20 km. Our goal is to study the strongest earthquakes in the region, and, since it is reasonable to assume that the whole volume till Moho is involved into the generation of such shocks (e.g. CAPUTO et al., 1973) the preferable thickness is defined by the Moho depth, i.e. 40 km. This is much larger than locked depth given in DISS, but significant seismicity extends till 40 km, % of instrumentally recorded earthquakes have focal depth $h \geq 20$ km, that proves seismogenic power of the dip structures in the region.

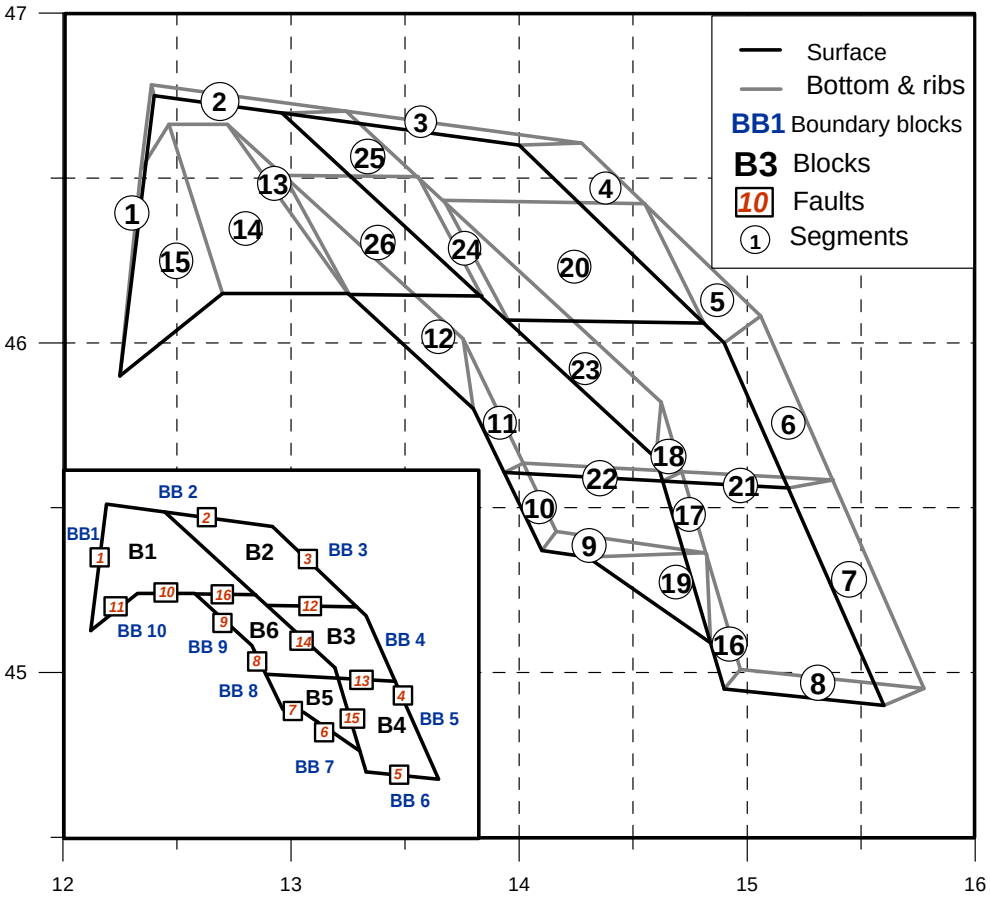

Fig. 3 Geometry of the block structure outlined on the base of the morphostructural map (GORSHKOV et al., 2004) and map of SS (DISS3.1.1, 2010). Numbers of faults, blocks and boundary blocks are given in the insert

To estimate the dip angles for the faults of the block structure we use the information from DISS3.1.1 (2010), and fault plane solutions (FPS) (GUIDARELLI, M. AND PANZA, 2006).We select the earthquakes in the vicinity of the faults of the block structure and determine the average dip angle for each fault. Many FPSs are available for the Southern boundary of the Alps (faults 10, 11, 16), Idrija line (fault 14) and the NW boundary of the structure (fault 1), while for some faults the FPS are very few or unknown. The dip angles are within limits given in DISS; the values are chosen to have smooth distribution on a given lineament (Table 2).

Table 2. Dip angles of faults.

Fault	*FPS*	*DISS*	*Model*	*Fault*	*FPS*	*DISS*	*Model*
1	89	-	88	9	62	40-85	70
2	86	-	85	10	34	30-40	35
3	69	-	70	11	35	30-50	35
4	60	-	70	12	-	-	45
5	-	-	80	13	90	-	85
6	-	45-60	60	14	70	70-85	70
7	-	-	80	15	-	-	80
8	-	70-85	80	16	47	30-45	45

The discretization of the fault segments is performed with cells whose linear size, ε=2 km, it allows us to model earthquakes with $M \geq 4$ (see eq. (6)).

The external velocities. Ten confining boundary blocks are introduced to prescribe the external motions acting in the region (Figure3). Velocities are defined by the GPS observations. We use

most recent and complete determination given by Cuffaro et al., (2010) and referred to the stable Eurasia, frame ITRF2005 (Altamimi et al. 2007). The velocities in the sites near structure boundaries, as well as prescribed velocities that we use while modeling are listed in the table 3.

Table 3. Velocities of boundary blocks in mm/yr.

BB	*Description*	*Observed GPS*			*Prescribed*	
		Site	*Vx (E)*	*Vy (N)*	*Vx (E)*	*Vy (N)*
1	Venetian Alps	AFAL	0.04	0.2	0.0	0.0
2	Periadriatic line	ACOM	0.24	0.29	0.4	0.25
		VLCH	1.05	0.77		
3	Austrian Alps	No	data		0.0	0.0
4	Dinarides/ Pannonian basin, N	No	data		-0.05	0.45
5	Dinarides/ Pannonian basin, S	No	data		-0.1	0.65
6	Dinarides	No	data		-0.25	1.25
7	Vinjdol-Rijeka	No	data		-0.35	2.50
8	Adria/Dinarides	TRIE	-0.43	2.00	-0.4	2.50
9	Friuli plain/Dinarides	PALM	0.02	2.04	-0.45	2.50
		MDEA	-0.39	2.11		
		UDIN	-0.17	1.99		
10	Friuli plain/Alps	CANV	0.06	0.79	0.0	1.5
		MPRA	0.15	1.66		
		PORD	-0.29	1.16		
		VENE	0.32	1.42		

GPS data are not available in the eastern boundary of studied region in the Austrian Alps, and in the Pannonian basin, and in the south, in Dinarides and Vinjdol-Rijeka. To prescribe velocities in these segments of the structure boundary we made a following assumption. 1. Velocities in the Alpine domain are very slow, and we prescribe zero velocities in the Austrian Alps (BB3). 2. Dinarides are involved in a NNW movement; that is proved by velocities in GSR1. We assume that the velocity in the Dinaric domain decreases from west to east, and that the eastern boundary of Dinarides undergoes some north-directed movement (BB4-BB6). Vinjdol-Rijeka (BB7) is a segment of the Adria boundary, that commonly moves northward, with velocities growing from north to south, and we propose its velocity similar to the ones in the Trieste site with a bit larger rate. The velocities in the boundary Dinarides/Friuli plain are prescribed a bit larger, than ones estimated by Cuffaro et al., (2010), as we can't ignore the results of another recent study, Bechtold et al. (2009), that find out a heightened velocity rate in Udine site relatively to ones in the other close sites, and that can't be explained by using of different reference system ITRF2000 (Altamimi et al. 2002).

Zero velocities are prescribed for the medium underlying all the blocks. While modeling and interpreting results we scale all the velocities to the one unit of model time, whose value will be derived in section below.

Rheology. The viscous-elastic properties are the same for all block's bottoms: elastic coefficient K=1.0 bar/cm, and coefficient controlling viscosity W=0.07 cm/bar. The viscous-elastic properties of the faults' segments depend on the rank of the corresponding morphostructural lineament (GABRIELOV et al., 1994). The high rank lineaments correspond to the wider and more fractured zones, so it is natural to assume that the rate of the inelastic displacements decreases with increasing rank of lineament: W is 0.08, 004, and 002 cm/bar in the segments of faults that correspond to the first, second and third rank lineaments, respectively. The special value W=0.16 cm/bar, is prescribed into two small segments, which are located in the highly fractured zones of

intersection of the large faults: triple junction zone of Adria, SE Alps and N Dinarides, and the intersection of Idrija line with the boundary between Alps and Dinarides. The DISS3.1.1 also proposes multiple seismogenic sources here, i.e. highly fractured zone. Value of Ws, that control change of rheology after an earthquake, is $1000 \times W$. We do not distinguish between the "locked" and "slipping" faults, as the fault's state can change with time, Gabrielov et.al. (1996) showed that Landers earthquake (California 1992) unlocked the fault system, and Northridge (California 1994) has locked in again. From the previous experience we know that block structure model never generates earthquakes in the all faults, so we obtain "locked" and "slipping" faults as one of the results of modeling without prescribing in advance some artificial parameters that restrict generation of synthetic events in the specific zones.
The standard values of the ratios of shear to normal stress (e.g. SOLOVIEV AND ISMAIL-ZADEH, 2003; PERESAN et al., 2007), that control earthquake occurrence in the model, are: B =0.10, H_f= 0.085, H_s = 0.07 and they are the same for all the segments. The list of the values is given in Table 4; the identification numbers of the segments are marked in Figure 3.

Table 4. Viscous-elastic parameters of fault's segments.

Segments	*K, bar/cm*	*W,cm/bar*	*W_s,cm/bar*
8, 17, 18, 23, 25	1.0	0.02	20
1-4, ,9, 19, 21, 22	1.0	0.04	40
5-7, 10-12, 14-16, 20, 26	1.0	0.08	80
13, 24	1.0	0.16	160

The relation of the chosen parameters with the physical features of the lithosphere can be derived from equations (2, 3). Assuming the width of the fractured zone a have an order of ~10km (D'Agostino, 2005) the effective shear modulus $\mu = aK = 10^5$ bar (10^{10} Pa), that is 3-5 times less than shear modulus in the Earth's lithosphere, and is in accordance with Fialko (2006), Barbot et al. (2009). The viscosity of the fault zones is estimated as $10^{18} \div 5 \times 10^{20}$Pa sec=$10^{13} \div 5 \times 10^{15}$bar sec (McCaffrey et al., 2000, Hacker et al., 1992), i.e. varies almost 3 order. As relative tectonic motion is slow in the studied region we assume the value of viscosity to be close to upper estimation, and $\eta \sim 10^{15} \div 10^{16}$ bar×sec. From (2) $\eta = a/W$, where η and W are related to one unit of the model time, so $\eta \sim 10^5/0.1 = 10^6$bar×unit of model time. With $\eta \sim 10^{15} \div 10^{16}$ bar×sec, we obtain one unit of model time ~ $10^9 \div 10^{10}$ sec that is ~30 ÷ 300 years. From the previous experience of modeling (e.g. Peresan et al., 2007) we suppose the unit of time is 150-250 years, and fix it as 200 years.

5. Results of modeling

The modeling has been carried out for 600 units of dimensionless time. Since the initial conditions correspond to zero stress and strain, beginning period of time is necessary for the system to reach regime behavior, thus we do not consider the first 100 units of time. We base the following analysis on the results obtained for 500 units of time, from 100 to 600. Accordingly to estimation above this period is equivalent to 75,000-125,000 years. Below we compare the result of modeling with available observation.

5.1 The Gutenberg-Richter relation.

We obtained 113077 synthetic earthquakes with $4 \le M \le 7.4$. The frequency-of-occurrence plot (Gutenberg-Richter plot) for the synthetic events is given in Figure 4, as well as the observed relation that is constructed from UCI catalog for the period 1870-2011 during which the catalog is representative for the events with $M \ge 4.0$. The plot for the synthetic seismicity is fairly linear in the range of magnitudes from 4.2 to 7.0 and has almost the same slope as the plot for the observed seismicity, as shown by the following best fit linear relations:

Observed: Log N = -0.96 M + 6.44; σ = 0.11

Synthetic: Log N = -0.97 M + 9.25; σ = 0.06

σ is standard deviation of the residual.
Since the b-values for observed and synthetic seismicity are the same, within the errors, we can check the real-time duration of the modeling T, by comparison of observed and modeled earthquake productivity as follows:

$T=10^{[(9.25-6.44)\pm 0.17]}\times 142$ yr $\approx 71000\div 118000 \times$ yr

This result fits to the estimation made in advance (section 4).

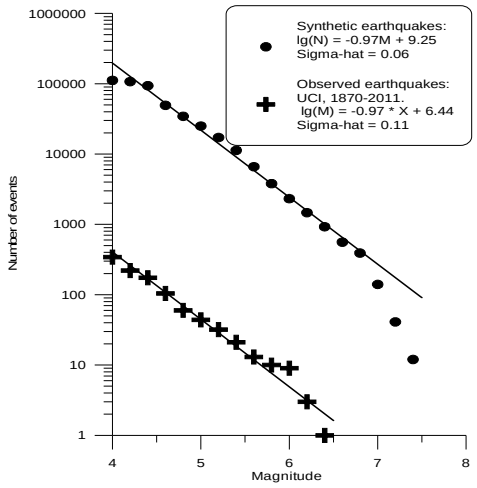

Fig. 4 Frequency-of-occurrence plots for observed and synthetic earthquakes and their fest-fit linear relations.

5.2 Movement in the block structure.

The velocities of the blocks obtained as a result of modeling, and the observed ones, where they are known (Cuffaro et al., 2010) are given in Table 5. We give two values of the modeled velocities, the average ones obtained as ratio of the total displacement, due to earthquakes and aseismic slip, to the total time period, and the velocities of aseismic slip. The general direction of the movement is N-NNE. The velocities in the Alpine domain (B1, B2) are very slow 0-3 0.4 mm/yr and they are clearly distinguished from ones in the Dinaric domain (B3-B6) where the rate is 1.2-2.0 mm/yr. The blocks westward of Idrija (B5, B6) move faster than the eastern ones (B3, B4). The velocity in Alps is in agreement with observations in the site AMPE. The velocity of the western Dinaric blocks (B3, B6) is similar to the observed one in site GSR1, while it is slower eastward to Idrija. The shortening rate of the Alpine domain is 1.2-1.5 mm/yr westward of Idrija and about 1.0 mm/yr eastward of Idrija. The overall displacement in the block structure obtained during the period of modeling is 2.0 mm/yr × 100000 yr ≈ 0.2 km, and with the linear size of the region 250-300 km, the strain is less than 10^{-3}, i.e. it is natural to neglect changes in the geometry of the fault system during the numerical simulation.

*Table 5.*Velocities of blocks in mm/yr

Block		*Observed GPS*		*Result of modeling*			
				Average		*Inter-seismic slip*	
	Site	*Vx, (E)*	*Vy, (N)*	*Vx, (E)*	*Vy, (N)*	*Vx, (E)*	*Vy, (N)*
B1	AMPE	0.03	0.32	0.02	0.32	0.02	0.36
B2				0.01	0.30	0.01	0.32
B3	GSR1	0.01	1.91	0.03	1.20	0.04	1.25
B4				-0.12	1.20	-0.10	1.21
B5				-0.13	1.45	-0.31	2.03
B6				0.01	1.48	-0.25	1.88

The aseismic slip rates and rakes in the individual segments are listed in the table 6. Slip velocity varies from 0.15 to 1.56mm/yr. The rake corresponds to the overthrast in the SE Alps/Friuli plain and SE Alps/N Dinarides boundaries, and right-lateral strike-slip with a small overthrast component in the Adria/N Dinarides, Idrija line and N Dinarides/Pannonian basin boundaries. The slip rate obtained as the result of modelling is similar to the upper estimation proposed in DISS or even a bit higher (Tab. 6). It can be explained as follows: the single segment in the

block model represents a zone of strain accumulation, and it summarizes slip that in reality is distributed in this zone among several faults. The rake is generally within limits given in DISS.

Table 6. Features of synthetic seismicity and modeled slip in the segments of the block structure and parameters of the corresponding seismogenic sources from DISS3.1.1 (2010).

Seg.	*N of Eq*	*Mmax*	*Mmax DISS*	*Slip mm/yr*	*Slip DISS*	*Rake*	*Rake DISS*	*Rake FPS*
1	2627	5.9	-	0.32	-	-3	-	-5
2	0	-	-	0.25	-	174	-	-
3	4241	6.6	-	0.25	-	172	-	170
4	8152	6.4	-	0.30	-	120	-	115
5	10963	7.0(1)*	-	0.8	-	112	-	115
6	4720	7.2(5)	-	0.8	-	147	-	125
7	0	-	-	0.55	-	153	-	-
8	0	-	-	0.15	-	181	-	-
9	314	6.9	-	0.47	-	135	-	105
10	608	6.8	5.5	0.47	0.1-0.5	176	160-180	140
11	517	7.2(4)**	5.5	0.62	0.1-0.5	166	160-180	140
12	10408	7.1(1)	5.5	0.62	0.1-0.5	148	120-180	135
13	9906	6.6	-	1.18	-	135	120-180	125
14	10685	7.0(2)	6.5	1.18	0.1-1	91	80-100	105
15	3047	7.1(16)	6.5	1.18	0.3-1.56	68	60-100	65
16	6040	6.4	6.2	0.15	0.1-0.5	146	80-140	140
17	933	5.7	-	0.78	-	173	-	150
18	653	5.3	-	0.64	-	187		155
19	7537	7.0(17)	6.0	0.47	0.2-0.5	123	100-140	125
20	6327	7.4(49)	-	0.92	-	92	-	95
21	0	-	-	0.14	-	178	-	-
22	0	-	-	0.15	-	152	-	-
23	1809	7.4((15)	6.8	0.64	0.1-0.5	153	160-180	130
24	1414	6.6	5.8	1.56	0.1-1	142	120-180	125
25	0	-	-	0.02	-	148	-	-
26	22828	7.2(30)	6.5	1.52	0.1-1.15	98	80-100	100

* Number of events with magnitude 7.0 and greater generated in the segment
**Largest earthquakes are multi-segment and occur in the segment10-11.

5.3 Regional-specific features of synthetic seismicity.

The spatial distribution of synthetic seismicity is shown in Figure 5. Detailed information about the number, maximum magnitude, and FPS of the synthetic events that occur along the different faults of the structure is given in Table 6.

The direct comparison of the relative seismic activity and of the Gutenberg-Richter relation with observations in the different territories is difficult, as it is impossible to assign, in a unique way, an observed event to a certain segment of the block structure. To overcome this difficulty we divide the study region into the ten sub-regions shown in Figure 5. Even if we model the seismicity for $M \geq 4$, we use the observed seismicity with $M \geq 3$ (UCI, 1870-2011) to obtain the more reliable estimation of the relative activity, since the number of recorded earthquakes with $M \geq 4$ is small, only 335 events. Results are given in the table 7.

The most active is sub-region 3, the zone of Alps-Dinarides-Adria junction. About half (45%) of the observed and 40% of the synthetic earthquakes are concentrated here. The number of synthetic earthquakes in the Vinjdol-Rijeka zone (sub-region 9) is more than two times larger

than the observed one, and we assume that it could be a consequence of the UCI incompleteness

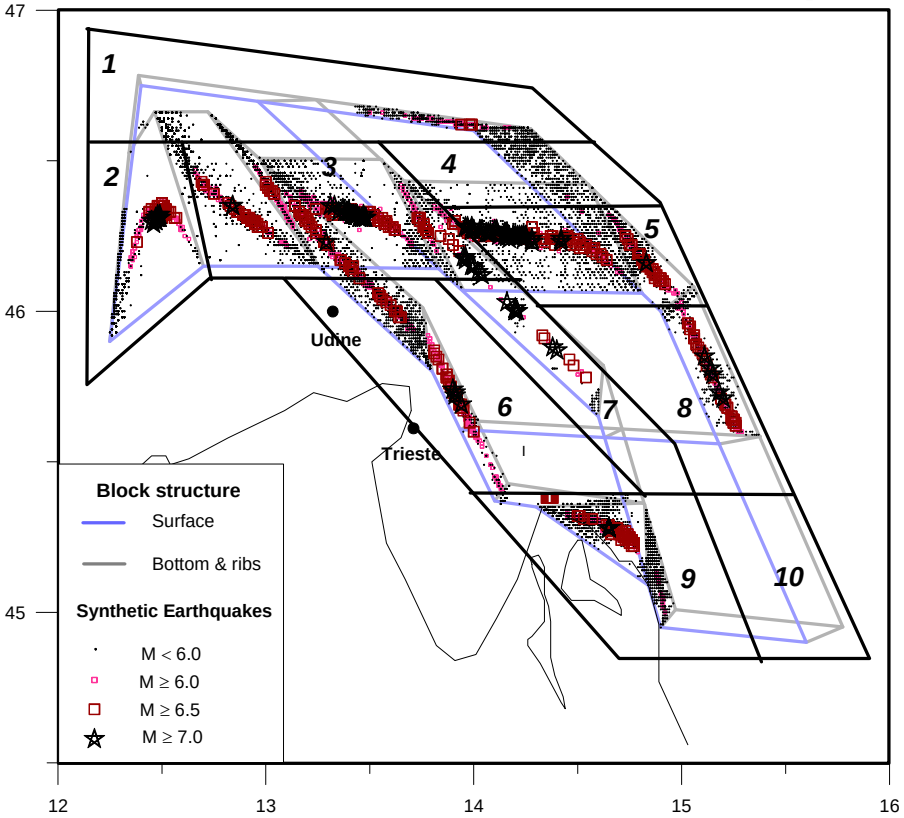

Fig. 5 Space distribution of the synthetic epicenters and ten sub-regions for comparison of synthetic and observed seismicity.

*Table 7.*Relative seismic activity in the different territories and slope of Gutenberg-Richter relation for observed and synthetic seismicity.

		Observed seismicity			*Synthetic seismicity*		
N	*Sub-region*	*Number of EQ*	*% of EQ*	*Slope of G-R plot*	*Number of EQ*	*% of EQ*	*Slope of G-R plot*
1	Periadriatic line	67	2.8	1.19±0.02	4241	3.7	1.24±0.11
2	Alps, western and southern boundary	333	13.8	0.77±0.02	5674	5.1	0.77±0.01
3	Junction zone Alps-Dinarides-Adria	1087	44.9	0.85±0.03	44833	39.7	0.95±0.02
4	Alps, eastern boundary	124	5.2	1.04±0.04	8152	7.2	1.50±0.07
5	Alps-Dinarides boundary	328	13.6	0.86±0.01	17290	15.3	0.87±0.01
6	Dinarides, western boundary, north	159	6.6	0.90±0.04	11533	10.2	0.92±0.09
7	Idrija line	121	5.0	0.96±0.02	2740	2.4	0.91±0.05
8	Dinarides, eastern boundary, north	111	4.6	1.03±0.05	4720	4.2	0.97±0.01
9	Dinarides, western boundary, south	123	5.1	0.85±0.05	14824	13.1	0.83±0.01
10	Dinarides, eastern boundary, south	3	0.1	-	0-	0.0	-

in this zone (see section 2). The model generates a relatively low number of events in two sub-regions: along Idrija line (sub-region 7), and in the western part of the boundary between Alps and Friuli plain (sub-region 2), nevertheless the synthetic earthquakes are very strong in these zones and the maximum magnitude reached is above 7. Therefore, even if there is some lack of small events, the level of synthetic seismicity is not low here. Since any large event with its aftershock sequence can change considerably the relative level of seismic activity in the zone where it occurs, we can consider the space distribution of synthetic seismicity is in agreement with the observations.

The slopes of the Gutenberg-Richter plots (*b*-value) for the observed and the synthetic seismicity (Table 7) are quite similar in the different parts of the region with the exception of sub-regions 3 and 4. The *b*-value is equal to 0.85±0.03 for the observed seismicity and 0.95±0.03 for the synthetic one at the junction zone SE Alps-N Dinarides-Adria (sub-region 3). This discrepancy can be connected with Friuli swarm of 1976, and if we exclude it from the catalog the *b*-value is 0.93±0.01, that is very close to one obtained from modeling 0.95±0.02. The *b*-values differ drastically in sub-region 4 (Alps, eastern boundary), probably because of the inadequate modeling of this area.

The FPSs for the synthetic events are summarized in Table 6: they indicate reverse faulting at the southern boundary of Alps (faults 11, 12, 16) that have a left-lateral strike-slip component in the western part (fault 11). Earthquakes in the Dinarides (faults 3-4, 6-9, 14) are the right-lateral strike-slips with a considerable reverse faulting component; along the Periadriatic line (fault 2) they are right-lateral strike-slips, and left-lateral strike-slip in the Venetian Alps (fault 1). It is in agreement with the available observations (Table 8).

Table 8. Comparison of synthetic and observed FPS (GUIDARELLI, M. AND PANZA, 2006)

Fault	*Synthetic FPS, average rake, degrees*	*Observed FPS, average rake, degrees*	*Fault*	*Synthetic FPS, average rake, degrees*	*Observed FPS, average rake, degrees*
1	-5	-4	9	135	142
2	-170	-179	10	105	95
3	115	112	11	65	78
4	125	97	12	95	-
5	-	-	13	-	-
6	125	-	14	130	148
7	107	-	15	140	-
8	140	-	16	100	72

The analysis of the result of the modeling can be summarized as follows: (1) velocities in the block structure are similar to those deduced from GPS data (Cuffaro et al.,2010), slip rate and rake in the faults is within limits proposed in DISS3.1.1, (2010); (2) the rate of tectonic velocities and the earthquake's productivity are in agreement; (3) the frequency-of-occurrence plot for the synthetic seismicity is linear and has the same slope, as that of the observed one; (4) the distribution of the synthetic epicenters recovers the main features of recorded seismicity; (5) the relative level of synthetic seismicity in the different parts of the region, as well as (6) synthetic FPS, do not contradict to the observations. We emphasize that the result of modeling is obtained without using any information about observed seismicity in the stage of the parameters determination.

6. Synthetic and observed strong seismicity: Discussion.

6.1. Maximum magnitude of synthetic earthquakes

The maximum magnitude of the synthetic earthquakes is 7.4. This value is larger than the maximum observed instrumental magnitude, 6.5 in 1976. Nevertheless the equivalent magnitude of instrumentally recorded Friuli series of 1976 is estimated above 7 (see section 2). A number of investigators report historical events with magnitude above 7. SHEBALIN et al. (1998) reports 7.9 in 1348, 7.4 in 1511 and 7.5 in 1690 (table 1). WESTAWAY (1992), on the base of the isoseismal maps of POSTPISCHL (1985b), estimates the magnitude of 1348 as 7.6, and 1511 as 7.0. Probably, the value of M=7.9 is overestimated, nevertheless, very likely the earthquakes of 1348 and 1511 had $M \geq 7$. Therefore, in spite of the absence of reliable instrumentally recorded data, one can conclude that the value of the maximum possible magnitude close to 7.5 is a realistic one.

6.2. Recurrence period of largest earthquakes over the whole region

The model generates 140 earthquakes with $M \geq 7$ during the period of 100,000 yr, i.e. 1-2 earthquakes per millennium. The time sequence of $M \geq 7$ earthquakes is given in Figure 6A together with the number of such earthquakes in a 1000 yr window, sliding with the step of 200 yr; the number varies from 0 to 6. The distribution of inter-event time is shown in Figure 6B: there is a small maximum in the time interval 0-300 yr, the distribution is quite homogeneous from 400 yr to 1200 yr, and maximum inter-event period lasts 2500 yr.

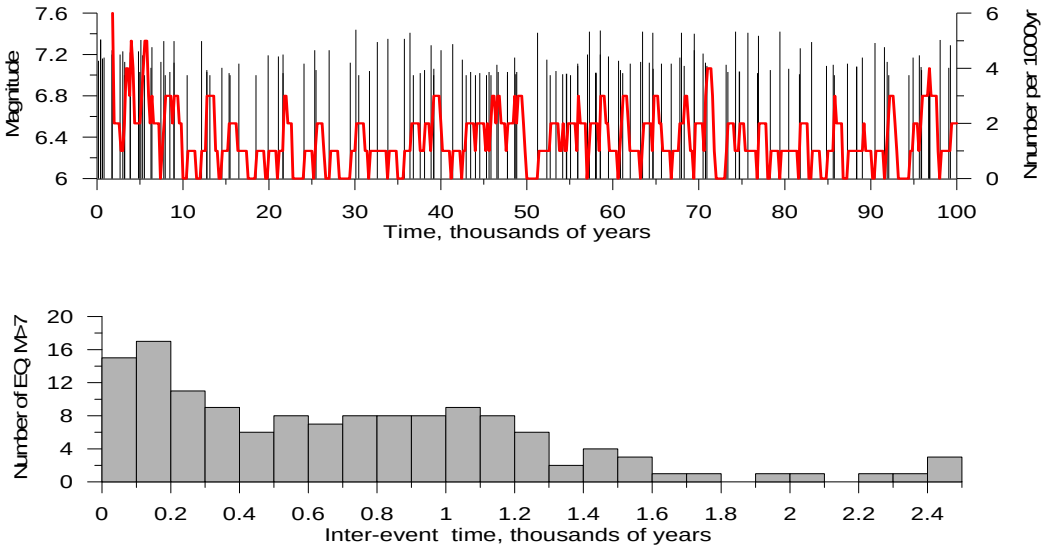

Fig. 6 A-Temporal sequence of the synthetic earthquakes with magnitude M≥7 (black bars) and number of synthetic earthquakes with magnitude M≥7 within a window of 1000yr sliding with step 200yr (red line); B - distribution of inter-event times for the synthetic earthquakes with magnitude M≥7

The results of the modeling do not contradict the available observation: SHEBALIN et al. (1998) report three extreme events during 1000 yr, in 1348, 1511 and 1690, with inter-event intervals of 163 yr and 179 yr, respectively, well in agreement with the values obtained from modeling. The fact that other investigators (PERESAN AND PANZA, 2002, GRUPPO DI LAVORO CPTI, 2004) do not report $M \geq 7$ earthquakes cannot be rejected by the results of modeling, because the synthetic catalogue contains long periods without extreme events.

6.3. Possible locations of strong events

The location of strong synthetic earthquakes is shown in the Figure 5. The results of modeling indicate that large earthquakes with $M \geq 6$ are generated everywhere excluding small territories in

the north-west and south-east of the region (segments 2, 7-8, 17-18), and in the transversal boundaries in the Alps (segment 25) and Dinarides (segments 21-22) (table 6).
The locations, maximum magnitude, and recurrence periods of the strongest synthetic earthquakes with $M \geq 7$ are summarized in the Table 9. Almost 70% of such events are generated along the southern boundary of the Alps, and 30% in the Dinaric domain. The most active is the boundary between Alps and Dinarides (table 9). The boundary between the Alps and Friuli plain is less active. Only two extreme events occur in Friuli segment (segment 14 in the model), with maximum magnitude 7.0. The analysis of synthetic seismicity behavior shows that almost all large earthquakes ($M \geq 6.0$) here occur in the clusters with typical duration of several moths; and the equivalent magnitudes (eq. (1)) of many clusters exceed 7. Recurrence period of such clusters is about 1-1.5 thousands of years. Natural seismicity demonstrates a similar behavior: an example is the Friuli sequence of 1976, when 4 earthquakes with $M \geq 6$ occurred within half a year with an equivalent magnitude about 7 (see section 2). The specific behavior of the observed seismicity at the Friuli segment can be explained by a high density of the seismogenic sources here (DISS3.1.1). The Block structure model reproduces this feature generating several moderate earthquakes instead of single large one, i.e. forming several seismogenic sources in the single model segment.
Many of the location of the synthetic M7+ earthquakes have been already experienced by large, $M \geq 6$, observed earthquakes (tables 1 and 9). Historical large events are unknown in the Western Dinarides near the city of Trieste where model has generated four M7 synthetic earthquakes (segments 10-11). Slejko et al., (2011) proposes seismogenic sources in the system of "silent" faults near Trieste, and estimate maximum possible magnitude 6.6 in faults traced very close to the model segments 10-11.
The observed historical earthquakes, candidates to be with $M \geq 7$, are the events of 1348, March, 1511 and 1690. On the basis of the results of the modeling we can propose the most probable locations and magnitudes for these three events (Table 10). The earthquake occurred in 1348 is characterized by the largest scatter in reported magnitude, which varies from 5.7 in UCI to 7.9 in ECCSE. The model confirms that, the magnitude can exceed 7, but it excludes the value $M=7.9$, since the obtained maximum is 7.4. The most realistic location of this earthquake is the boundary between Alps and Dinarides (UCI, PERESAN AND PANZA, 2002) where the maximum number and magnitude of synthetic events are obtained. If we accept that the magnitude of 1348 quake is greater than 7, then the location at the Periadriatic line (SHEBALIN et al., 1998; POSTPISCHL, 1985a) is rejected since the maximum synthetic magnitude is 6.6 here. The location at the Friuli segment, given in CPTI and in HAMMERL (1994), is less probable as only 2 synthetic earthquakes with $M=7$ are obtained here.
The locations of earthquakes of 1511, March, and 1690 are similar in all considered catalogs. All of them report the epicenter of 1511 close to the north of the Idrija, and the epicenter of 1690 at the eastern segment of the Periadriatic line. The reported magnitudes for the 1511 earthquake are 5.7 (UCI), 6.5 (CPTI), 6.9 (NEIC) and 7.4 (ECCSE), and $M=5.7$ seems to be a real underestimation. The magnitudes reported for the 1690 quake are 5.2 (UCI), 6.0 (CPTI), 7.5 (ECCSE) while NEIC gives no value. The modeling supports these locations for both epicenters. The value $M=7.0\pm0.5$ seems realistic for the earthquake of 1511, while for the earthquake of 1690 the value $M=7.5$ (ECCSE) is rejected, since, at the Periadriatic line, the maximum magnitude is 6.6, and $M=6.0\pm0.5$ is a more reliable value.

Table 9. Locations and magnitudes of observed earthquakes consistent with the results of modeling

Earthquake, date	*Location of epicenter*	*Estimation of magnitude*
1348	Boundary between Asps and Dinarides	7.0÷7.5
1511, March	Idrija	7.0±0.5
1690	Eastern segment of Periadriatic line	6.0±0.5

7. Comparison of the results of block structure modelling and DISS.

The DISS3.1.1 is the most detailed and complete data base of the seismogenic sources, maximum possible magnitudes and recurrence period of the strongest earthquake in the studied region. We compare the result of the block structure modelling with DISS data.

1. Almost all seismogenic sources (SS) from DISS (excluding Medea that is out of the territory of the MSZ (Gorshkov et al., 2004)) fit to the outlined block structure, their positions, strike, and dip angles corresponds to the model parameters (Fig. 1, Tab 2). The slip rates obtained from the modelling are close to upper estimation of slip rates given in DISS; and their values correlate well: a higher modelled slip rate corresponds to the higher slip rate in SS (Tab. 6). The modelled slip rake is commonly in accordance with DISS (Tab 6).

2. We obtain synthetic earthquakes with magnitude more than 6 in all SS from DISS included in the block structure. Synthetic strong earthquakes also occur in the territories that are not included into DISS as potential seismogenic sources. We suppose that some of them are out of DISS territory, e.g. boundary between Dinarides and Pannonian basin, European data base "Faust" contains seismogenic sources here and at the east of Periadriatic line. A number of the potential SS is proposed by Slejko et al. (2011) at the "silent" faults in the north of the Adria, where DISS do not place SS. We obtain the strongest earthquakes in the boundary between Alps and Dinarides eastward of Idrija, where DISS do not places any SS. High slip rate in this zone that we obtain from modelling are confirmed by GPS observation: the northward velocities are relatively high in the Dinarides and very slow in Alpine domain (Cuffaro et al., 2010). Results of modelling proposes that boundary between SE Alps and Dinarides is a zone of the strain accumulation, where "silent" slipping periods alternate with seismically active ones, and typical duration of aseismic periods is about 1000 years, and sometime reaches 2000 years. Probably, this zone is in the "slipping" state now, but it can switch to the active seismic state in the future.

3. The values of maximum magnitude obtained from modelling are systematically higher than ones given in DISS (Tab. 6). One of the possible causes of this discrepancy is considerable larger depth and model simplification that supposes fixed with depth rheological parameters. It leads to the growth of the area of the potential SS, and consequently larger maximum magnitude. Our attempts of modelling with lesser depth were unsuccessful – synthetic seismicity fits poorly to the observation with reasonable variation of the input parameters. It indicates that deep structures are significantly involved into the seismogenic process and influence considerably the process of strain and stress transfer and accumulation.

Another cause of discrepancy in maximum magnitudes can be explained as follows. Single segment in the block model represents the fault zone with many SS, i.e. largest earthquake in the single model segment can be interpreted as multi-segment natural earthquake. More than, some large synthetic events expand more than one model segment; e.g. events with magnitude 7.0 generated near the city of Trieste are multi-segment ones and occur in the segments 10, 11. The maximum magnitudes in DISS are determined under assumption that strongest earthquake raptures the single segment. This approach was introduced by Coppersmith and Schwartz (1984). Nevertheless, segments may also rapture in cascades producing larger earthquakes than the characteristic events in the single segments, as occurred in the Landers, California, earthquake (Wald and Heaton 1994). In California multiple-segments ruptures were included in the hazard calculation (Frankel et al, 1996). One can't exclude multi-segment earthquake in the studied region, thus maximum magnitude can occur larger than given in DISS.

The recent estimation of the maximum magnitude given by Slejko et al. (2011) are, in some faults, considerably larger than ones from DISS, e.g. Mmax(DISS) is 5.5 in SICS004, SICS005 in the western boundary of Dinarides, while Mmax(Slejko) is 6.6 in the fault 8c and 12 situated in this zone. These values are much close to the ones obtained from the modelling.

4. The comparison of the recurrence periods proposed by DISS and obtained from the modelling is difficult as the maximum magnitudes differ significantly; single segment in the model

represents a set of SS described in DISS. The recurrence periods of the strongest events in the single model segments vary from thousands to tens thousands of years that seems a realistic times.
Summarizing the results of analysis given above we do not see a severe contradiction between DISS data and output of the modelling in the junction zone of SE Alps and Dinarides.

8. Conclusions

We use the block structure model to study long-term (100,000 yr) characteristics of strong seismicity in the Alps-Dinarides junction zone. The model recovers the main features of observed seismicity and kinematics in the region. The rates and directions of the tectonic movements are in agreement with GPS observations, and slip rates and rakes are similar to ones given in DISS. The distribution of epicenters, *b*-value, relative levels of seismic activity in the different parts of the region as well as fault plane solutions are similar for recorded and synthetic earthquakes.
The synthetic earthquakes with magnitude $M \geq 7$ do not fit to the linear part of the frequency-of-occurrence plot thus can be considered as extreme events. The average rate of such earthquakes is a bit 1- 2 events per 1000 yr, and the maximum magnitude of the synthetic earthquakes is 7.4, not in contradiction with the available historical observations.
Most of the extreme synthetic events sit at the southern boundary of the Alps, where the highest level of recorded seismic activity is observed. Another large group of extreme events is found along the Adriatic coast, to the east of Istria peninsula. Several synthetic earthquakes with $M \geq 7$ are generated on Idrija line and at the eastern and western boundaries of Dinarides, that have experienced real earthquakes with $M > 6$. The results of modeling outline a number of possible locations of extreme events where large earthquakes have not yet been observed, in particular there are four extreme events near Trieste, at the western boundary of Dinarides. The underestimation of the recorded information with respect to the results of the modeling is not surprising when considering that seismogenetic tectonic processes act for time intervals much longer than 1000 yr, the maximum duration of any reliable catalogue of strong earthquakes.
The results of modeling do not contradicts severely do the DISS data. Slip rates and rakes are in agreement with ones given in DISS. Earthquakes with magnitudes more than 6 are generated in the all SS included in the block structure. The larger than in DISS maximum magnitudes of synthetic events could be obtained (i) as single segment in the model represent the fault zone i.e. entire set of SS, so the largest synthetic earthquakes are interpreted as multi-segment ones; (ii) recent studies, e.g. Slejko et al. (2011), proposes larger maximum magnitudes. We also obtain realistic recurrence periods of strongest events in the individual segments that last from thousands to tens of thousands years.
Even if the assumption that external tectonic movements are stationary cannot be verified, due to the very short period of time for which GPS observations are available, the model reproduces many features of the actual regional seismicity and kinematics. Therefore the present study gives estimates of the maximum magnitude, recurrence time, and possible locations of the largest earthquakes at the junction zone between SE Alps and N Dinarides that can be taken into account in seismic hazard and risk assessment. We propose that block structure modeling of the largest earthquake may be useful in other seismically dangerous regions where data base similar to DISS does not exist.

Reference

Altamimi Z, Collilieux X, Legrand J, Garayt B, Boucher C (2007) ITRF2005: a new release of the International Terrestrial Reference Frame based on time series of station positions and Earth Orientation Parameters. J Geophys Res 112. doi:10.1029/2007JB004949

Altamimi, Z., Sillard, P., and Boucher, C.: ITRF2000: A new release of the International Terrestrial Reference Frame for Earth science applications, J. Geophys. Res., 107(B10), 2214, (2002), doi:10.1029/2001JB000561

Barbot, S., Fialko, Y., and Sandwell, D. Three-dimensional models of elastostatic deformation in heterogeneous media, with applications to the Eastern California Shear Zone. Geophys. J. Int. 179, 500-520 (2009)

Basili R., G. Valensise, P. Vannoli, P. Burrato, U. Fracassi, S. Mariano, M.M. Tiberti, E. Boschi (2008), The Database of Individual Seismogenic Sources (DISS), version 3: summarizing 20 years of research on Italy's earthquake geology, *Tectonophysics*, doi:10.1016/j.tecto.2007.04.014

Bechtold, M., M. Battaglia, D. C. Tanner, and D. Zuliani (2009), Constraints on the active tectonics of the Friuli/NW Slovenia area from CGPS measurements and three-dimensional kinematic modeling, J. Geophys. Res., 114, B03408, doi:10.1029/2008JB005638.

Borghi, A., Aoudia, A., Riva, R., and Barzaghi, R. GPS monitoring and earthquake prediction: A success story towards a useful integration. Tectonophysics 405, p177-189, (2009)

Burrato, P., M. E. Poli, P. Vannoli, A. Zanferrari, R. Basili and F. Galadini. 2008 Sources of Mw 5+ earthquakes in northeastern Italy and western Slovenia: an updated view based on geological and seismological evidence. Tectonophysics, 453, 157-176, 10.1016/j.tecto.2007.07.

CAMASSI, R., AND STUCCHI, M.: NT 4.1 un Catalogo Parametrico di terremoti di Area Italiana al di sopra della soglia di danno, CNR-GNDT. http://emidius.mi.cnr.it/NT/home.html/ (1996)

CAPUTO, M., KEILIS-BOROK, V., KRONROD, T., MOLCHAN, G., PANZA, G.F., PIVA, A., PODGAEZKAYA, V. AND POSTPISCHL, D.: Models of earthquake occurrence and isoseismals in Italy. Ann. Geof., **26**, 421-444 (1973)

CHIMERA, G., AOUDIA, A., SARAÒ, A., AND PANZA, G. F.: Actives tectonics in Central Italy: constraints from surface wave tomography and source moment tensor inversion. Phys. Earth Planet. Inter. 138, 241-262 (2003)

CLOETINGH, S., TORNU, T., ZIEDLER, P.A., BEEKMAN, F.: Neotectonics and intrapalte topography of the northern Alpine Foreland. Earth-science Reviews **74,** 127-196 (2006)

Coppersmith, K.J., and Schwartz, D.P.: Introduction to the Special Section on Fault Behavior and Eartquake Generation Process. JGR, 89 B7, pp. 5669-5673 (1984)

CUFFARO, M., CARMINATI, E. AND DOGLIONI, C.: Horizontal versus vertical plate motions. eEarth Discuss. **1**, 63–80. www.electronic-earth-discuss.net/1/63/2006/ (2006)

Cuffaro, M., Riguzzi, F., Scrocca, D., Antonioli F., Carminati, E., Livani M., Doglioni, C. : On the geodynamics of the northern Adriatic plate. Rend. Fis. Acc. Lincei, Springer –Ferlag (2010), doi 10.1007/s12210-010-0098-9

D'Agostino, N., Cheloni, D., Mantenuto, S., Selvaggi, G., Michelini, A., and Zuliani, D.: Strain accumulation in the southern Alps (NE Italy) and deformation at the northeastern boundary of Adria observed by CGPS measurements. Geophysical Research Letters. **32**, L19306, doi:10.1029/2005GL024266 (2005)

D'AMICO, V., ALBARELLO, D. AND MANTOVANI, E.: A distribution-free analysis of the magnitude-intensity relationship: an application to the Mediterranean region, Ann. Geophys., Suppl IV, **16**, 1192 (1998)

DISS Working Group (2010). Database of Individual Seismogenic Sources (DISS), Version 3.1.1: A compilation of potential sources for earthquakes larger than M 5.5 in Italy and surrounding areas. http://diss.rm.ingv.it/diss/

Fialko, Y. Interseismic strain accumulation and the earthquake potential on the southern San Andreas fault system. Nature 441,968-971, (2006) doi:10.1038/nature04797

FITZKO, F., SUHADOLC, P., AOUDIA, A., PANZA, G.F.: Constraints on the location and mechanism of the 1511 Western-Slovenia earthquake from active tectonics and modeling of macroseismic data. Tectonophysics, **404**, 77– 90 (2005)

FRANKEL, A., MUELLER, C., BARNHARD, T., PERKINS, D., LEYENDECKER, E.V., DICKMAN, N., HANSON, S., AND HOPPER, M.: National Seismic Hazard Maps: Documentation June 1996. USGS Open-File Report 96-532 (1996). http://pubs.usgs.gov/of/1996/532/

Hacker, B. R., A. Yin, J. M. Christie, and G. A. Davis (1992), Stress magnitude, strain rate, and rheology of extended Middle Continental Crust inferred from quartz grain sizes in the Whipple Mountains, California, *Tectonics*, 11(1), 36–46, doi:10.1029/91TC01291.

GUIDARELLI, M. AND PANZA, G.F.: INPAR, CMT and RCMT seismic moment solutions compared for the strongest damaging events (M_4.8) occurred in the Italian region in the last decade. Rend. Accad. Naz. delle Scienze detta dei XL Mem. Di Scienze Fisiche e Naturali, 30, 81-98 (2006).

GABRIELOV, A. M., KOSOBOKOV, V. G., AND SOLOVYEV, A. A.: Numerical simulation of block structure dynamics. In KEILIS-BOROK, V.I. (ed.) Seismicity and Related Processes in the Environment. Research and Coordinating Centre for Seismology and Engineering, Moscow. **1**, 22-32 (1994)

GABRIELOV, A. M., KEILIS-BOROK, V., AND JACKSON D.D.: Geometric incompatibility in a fault system. Proc. Natl. Acad. Sci. USA, 93, 3838-3842. (1996)

GABRIELOV, A. M., LEVSHINA, T. A., AND ROTWAIN, I. M.: Block model of earthquake sequence. Phys. Earth Planet. Inter. **61**, 18-28 (1990)

GORSHKOV, A.I., PANZA, G.F., SOLOVIEV, A.A., AOUDIA, A.: Identification of seismogenic nodes in the Alps and Dinarides. Bolletino della Societa Geologica Italiana, **123**, 3-18 (2004)

GORSHKOV, A.I., PANZA, G.F., SOLOVIEV, A.A., AOUDIA, A., PERESAN, A.: Delineation of the geometry of the nodes in the Alps-Dinarides hinge zone and recognition of seismogenic nodes ($M \geq 6$). Terra Nova, **21**, No. 4, 257–264 (2009)

GRUPPO DI LAVORO CPTI: Catalogo Parametrico dei Terremoti Italiani, versione 2004 (CPTI04). INGV, Bologna, http://emidius.mi.ingv.it/CPTI04/ (2004)

Hacker, B.R., Yin, A., Christie, J.M., and Davis G.A.: Stress magnitude, strain rate, and rheology of extended middle continental crust inferred from quartz grain sizes in the whipple mountains, California. Tectonics, vol. 11, no. 1, pages 36-46, (1992)

HAMMERL, C.: The earthquake of January 25th, 1348: discussion of sources. In: P. ALBINI AND A. MORONI (eds.) Historical investigation of European earthquakes. C.N.R. 1st.Ric. Rischio Sism., Milano (1994)

ISMAIL-ZADEH, A., LE MOUËL, J.-L., SOLOVIEV, A., TAPPONNIER, P., AND VOROBIEVA, I. Numerical modeling of crustal block-and-fault dynamics, earthquakes and slip rates in the Tibet-Himalayan region. EPSL, **258**, 3-4, 465-485 (2007)

Keilis-Borok, V. I., Rotwain, I. M., and Soloviev, A. A. (1997), Numerical modelling of block structure dynamics: dependence of a synthetic earthquake flow on the structure separateness and boundary movements, J. Seismol. *1*, 151-160.

McCaffrey, R., Zwick, P.C., Bock, Y., Prawirodirdjo, L., Genrich, J.F., Stevens,C.W., Puntodewo, S.S.O., and Subarya C.: Strain partitioning during obligue plate convergence in northern Sumatra: Geodetic and Seismologic constraints and numerical modeling. JGR 105, NoB12, pp 28,363-28,376 (2000)

NEIC Hypocenter data file. http://neic.usgs.gov

PANZA, G. F., RAYKOVA, R. B.: Structure and rheology of lithosphere in Italy and surrounding. Terra Nova, **20**, 194–199 (2008)

PERESAN, A., PANZA, G. F.: UCI2001: The Updated Catalogue of Italy, ICTP, Trieste, Internal report, IC/IR/2002/3, and its updates. (2002)

PERESAN, A., VOROBIEVA, I., SOLOVIEV, A., PANZA, G.F.: Simulation of Seismicity in the Block-structure Model of Italy and its Surroundings. Pure Appl. Geophys., **164**, 2193-2234 (2007)

POSTPISCHL, D.: Catalogo dei terremoti Italiani Dall'Anno 1000 al 1980. Consiglio Nazionale delle Richerche, Rome, Italy, 1985. 239 (1985A)

POSTPISCHL, D.: Atlas of isoseismal maps of Italian Eartquakes. Consiglio Nazionale delle Richerche, Rome, Italy, 1985. 164 (1985B)

Rundle, J.B., Rundle P.B., Donnellan, A., Li, P., Klein, W., Morein, G., D. Turcotte, L., Grant, L.; Stress transfer in earthquakes, hazard estimation and ensemble forecasting: Inferences from numerical simulations. Tectonophysics, 413 109–125 (2006)

SHEBALIN, N., LEYDECKER, G., MOKRUSHINA, N., TATEVOSIAN, R., ERTELEVA, M., & VASSILIEV, V.: Earthquake catalogue for Central and Southeastern Europe 342 BC - 1990 AD. European Commission, Report No. ETNU CT 93-0087, Brussels (1998).

Sadovskii, M.A.: Block structure of the Earth's lithosphere. *Sov. Phys. Usp.*, **28** 937 (1985) doi:10.1070/PU1985v028n10ABEH003953.

Slejko, D., Carulli, G.B., Carica, J., and Santulin, M. The contribution of "silent" faults to the seismic hazard of the northern Adriatic Sea. Journal of Geodynamics 51, 166-178, (2011)

SOLOVIEV, A., ISMAIL-ZADEH, A.: Models of dynamics of block-and-fault systems, In KEILIS-BOROK, V. I., AND SOLOVIEV, A. A. (eds.) Nonlinear Dynamics of the Lithosphere and Earthquake Prediction, pp 71-139. Springer-Verlag, Berlin-Heidelberg (2003)

Soloviev, A. A, Vorobieva, I. A., and Panza, G. F. (1999), *Modelling of block-structure dynamics: Parametric study for Vrancea*, Pure Appl. Geophys. *156*, 395-420.

SUHADOLC, P., PANZA, G.F., MARSON, I., COSTA, G. AND VACCARI, F.: Analisi della sismicita' e meccanismi focali nell'area italiana. Atti Convegno Pisa GNDT, **1**, 157-168 (1992)

Utsu, T. and SekiI, A. (1954), A relation between the area of aftershock region and the energy of main shock, J. Seismol. Soc. Japan 7, 233–240.

Vannoli, P., S. Barba, R. Basili, P. Burrato, U. Fracassi, V. Kastelic, M.M. Tiberti and G. Valensise. 2009. Seismogenic sources in northeastern Italy and western Slovenia: an overview from the Database of individual Seismogenic Sources (DISS 3.0.4). Rendiconti online Serv. Geol. It., 5, 227-229.

Wald, D.J., and HeatonT.H.: Spatial and Temporal Distribution of Slip for the 1992 Landers, California, Eartquake. Bulletin of the Seismological Society of America, 84, 3, pp. 668-691 (1994)

Wells, D.L., and Coppersmith, K.J. New Empirical Relationships among Magnitude, Rupture Length, Rupture Width, Rupture Area, and Surface Displacement. Bulletin of the Seismological Society of America, 84, 4, 974-1002. (1994)

WESTAWAY, R.: Seismic moment Summation for Historical Eartquakes in Italy: Tectonic Implications. Journal of Geophysical research. **97**, No B11, 15,437-15,464 (1992)

ŽIVČIČ, M., SUHADOLC, P., VACCARI, F.: Seismic zoning of Slovenia based on deterministic hazard computations. Pure Appl. Geophys. **157**, 171– 184 (2000)